

## Research Article

# Research on Scheduling Algorithm of Agricultural Machinery Cooperative Operation Based on Particle Swarm Neural Network

Wei Li 

*Jiangsu Food and Pharmaceutical Science College, Huai'an 223003, China*

Correspondence should be addressed to Wei Li; 19991004@jsfpc.edu.cn

Received 17 February 2022; Revised 12 March 2022; Accepted 18 March 2022; Published 8 April 2022

Academic Editor: Qiangyi Li

Copyright © 2022 Wei Li. This is an open access article distributed under the Creative Commons Attribution License, which permits unrestricted use, distribution, and reproduction in any medium, provided the original work is properly cited.

In order to improve the cooperative operation scheduling effect of agricultural machinery, this article uses particle swarm neural network to study the cooperative operation scheduling algorithm of agricultural machinery and improves the cooperative scheduling effect of intelligent agricultural machinery. Aiming at the mixed integer nonlinear programming problem, this article proposes a collaborative algorithm of population intelligence and linear programming. The outer layer of the algorithm uses the improved particle swarm algorithm IPSO module, the inner layer uses the simplex algorithm SIM module, and the optimal solution of the MINLP problem is obtained through the iterative update of the inner and outer modules. The experimental study shows that the cooperative operation scheduling model of agricultural machinery based on particle swarm neural network proposed in this article can play an important role in modern agricultural planting and effectively improve the efficiency of agricultural planting.

## 1. Introduction

China is a big agricultural country with a vast territory, complex geographical environment, and different natural conditions, and agricultural production has obvious regional and time differences. In particular, in recent years, with the process of rural urbanization and the introduction of policies such as the state's encouragement of migrant workers to work in cities, most young and middle-aged laborers have gone out to work. However, women and the elderly stay behind in the countryside, so farmers have more urgent requirements for agricultural mechanization, and the demand for agricultural machinery operations is very high. The supporting role of agricultural mechanization in the construction of modern agriculture is becoming increasingly important. The experience of developed countries shows that agricultural mechanization is an important carrier for improving the level of agricultural science and technology and equipment, and an important force for accelerating agricultural modernization. China is a country with a large population and relatively little land, and the income level of farmers is low.

Due to the generally high price of agricultural machinery, ordinary farmers cannot afford to buy them. Users with agricultural machinery must not only complete harvesting tasks for themselves, but also complete harvesting tasks for more farmers through reasonable configuration. At the same time, they also need to consider how to obtain more economic benefits and obtaining greater economic benefits has become the decision-making goal of policy makers.

This article combines the particle swarm neural network to study the cooperative operation scheduling algorithm of agricultural machinery to improve the cooperative scheduling effect of intelligent agricultural machinery, which provides a theoretical reference for the further development of agricultural intelligence.

## 2. Related Work

The literature [1] proposed a special operation method for the VRP problem in the agricultural field to solve the planning and scheduling problems of field operations and achieved good results in the scheduling of various types of agricultural operations. Literature [2] established a relatively

complete mathematical model of agricultural machinery continuous operation scheduling. The model includes input, data preprocessing, scheduling, and output. The output results include the Gantt chart of agricultural machinery operations and the estimated cost of the scheduling scheme. Solve the problem of continuous operation scheduling of agricultural machinery. Reference [3] combined neural network (NN) and genetic algorithm (GA) to optimize the path of agricultural robots. The motion recognition of complex agricultural robot nonlinear systems is achieved through the high learning ability of NN. The optimal path is obtained by genetic algorithm, and the path is continuously optimized through selection, crossover, and mutation. The study not only considers the optimization objective of the shortest path, but also optimizes the steering angle and total transfer time. Literature [4] improved the BRUSPLAN model based on the idea of integer programming and established a two-stage stochastic linear programming model for the planting of vegetable crops. Because there are many uncertain factors in agriculture, the deterministic model often cannot play a very good role, and the model considers various uncertain factors in agriculture, reducing the uncertainty in agriculture such as temperature, precipitation, and other uncertainties for agricultural production. At the same time, risk factors are considered, risk control is carried out, and the benefits of vegetable cultivation are further improved through risk control. Reference [5] established a linear programming model for crop harvesting operations. The model considered resource constraints and operation time constraints and proposed two heuristic algorithms to solve the problem. The first method takes the operation rate as the primary optimization objective, and the second method takes the operation completion rate as the main optimization goal. This method meets the time window requirements as much as possible and optimizes the start time of each job. The calculation results show that the algorithm can quickly provide an optimization scheme to solve the problem of rapeseed harvest scheduling. Reference [6] used greedy algorithm and tabu search algorithm to optimize the dispatching path of agricultural machinery. The scheduling model takes into account job delays due to factors such as limited equipment and staff. Using commercial integer programming software to solve the problem, a feasible scheduling scheme can be solved within a reasonable calculation time. Reference [7] divided the agricultural machinery scheduling process into four independent steps: agricultural machinery allocation, farmland area coverage, agricultural machinery scheduling path generation, and secondary adjustment of the scheduling scheme. Among them, in the step of generating the dispatching path of agricultural machinery, a mathematical model based on the vehicle dispatching problem is proposed, which is solved by heuristic algorithm and genetic algorithm. Compared with the vehicle scheduling problem, there are more uncertain factors in the agricultural machinery scheduling problem, and the optimal scheduling scheme must be generated dynamically and in real time during the operation process. The dynamic agricultural machinery scheduling problem needs further research. The literature

[8] studied the minimization of nonoperation mileage (i.e., the transfer distance, excluding the mileage when operating within the farmland) in the process of agricultural machinery scheduling. The problem is regarded as a binary integer programming problem, and the path is optimized by calculating the traversal sequence of parallel paths.

Reference [9] proposed a two-stage meta-heuristic algorithm combining simulated annealing algorithm, genetic algorithm, and hybrid Petri network model to optimize the allocation and scheduling of agricultural machinery resources. In the first stage, the simulated annealing algorithm is used to optimize the scheme of allocating resources; in the second stage, the genetic algorithm is used to determine the priority of the jobs and generate the agricultural machinery scheduling scheme according to the hybrid Petri network model. The two-stage method allocates job tasks first and then enters into job priority sorting and scheduling, so that resources are independent of each other, which avoids deadlock and improves the efficiency of the algorithm. The model does not consider uncertain constraints such as weather and mechanical failures and is not suitable for dynamic operations. Reference [10] conducted a detailed study and classification of agricultural machinery operation scheduling to abstract the common characteristics of different operation scenarios, establish a connection with traditional vehicle scheduling problems, and distinguish between agricultural machinery scheduling problems and vehicle scheduling problems with time windows. Most agricultural machinery operations are complex, especially continuous operations, which involve the collaborative operation of multiple types of agricultural machinery, and the scheduling of different types of agricultural machinery has higher requirements in terms of time sequence. Reference [11] studied the dynamic agricultural machinery scheduling problem with uncertain factors and proposed an abstract two-dimensional grid, which creates discrete transition nodes in the grid state space. Generate optimal paths using a graph search algorithm. This algorithm improves the operation efficiency of agricultural machinery, and the algorithm has high computational efficiency and is suitable for many types of agricultural machinery to participate in large-scale dynamic agricultural machinery scheduling problems at the same time. In reference [12], aiming at the problem of cross-farm operation of agricultural machinery, integrating optimization objectives such as time and space, an agricultural machinery scheduling model is established, the problem is represented by the graph theory method, and the Dijkstra algorithm is used to solve the single-source path planning problem. The model proposed in this article is ideal, the solution speed is fast, but the adaptability to the scene is limited. Reference [13] explored a large number of agricultural contracting cases and established an agricultural machinery scheduling model based on the traveling salesman variant model with a time window. The ant colony algorithm is selected to iteratively optimize the scheduling path, and the algorithm characteristics are very suitable for parallel implementation, thereby improving the computing efficiency. Reference [14] regarded the agricultural machinery scheduling problem as a vehicle routing problem with a time

window and proposed a job scheduling method that is suitable for relatively scattered and random spatial distribution. The method is divided into three stages: the first stage preprocesses the input data, the second stage evaluates the time of all operating points, and the third stage uses the greedy algorithm and the tabu search algorithm to conduct agricultural machinery based on the results obtained in the first two stages Optimization of scheduling, where tabu search avoids getting stuck in local optima by employing neighborhood search techniques. Reference [15] used the saving algorithm to construct the agricultural machinery scheduling path, considered the problem of single vehicle type and multi-vehicle type at the same time, and simulated the random agricultural machinery scheduling scenario and the dynamic agricultural machinery scheduling scenario. The algorithm is outstanding in minimizing the cost of agricultural machinery transfer.

### 3. Particle Swarm Neural Network Algorithm

The general model of mixed integer nonlinear programming problem is as follows:

$$\begin{aligned} & \min f(x_1, x_2, x_3, y) \\ & \text{s.t. } g(x_1, x_2, x_3, y) \leq 0 \\ & h(x_1, x_2, x_3, y) = 0 \\ & x_1 \in X_1, x_2 \in X_2, x_3 \in X_3, y \in Y. \end{aligned} \quad (1)$$

Among them,  $x_1$  represents a strong nonlinear continuous variable,  $X_1 \in R^{l_1}$ ,  $l_1$  is the dimension ( $l_1$  is an integer greater than or equal to 0).  $x_2$  represents a linear continuous variable,  $X_2 \in R^{l_2}$ ,  $l_2$  is the dimension ( $l_2$  is an integer greater than or equal to 0).  $x_3$  represents a weak nonlinear continuous variable,  $X_3 \in R^{l_3}$ ,  $l_3$  is the dimension ( $l_3$  is an integer greater than or equal to 0).  $y$  represents an integer variable,  $Y \subset N^{l_4}$ ,  $l_4$  is the dimension ( $l_4$  is an integer greater than 0).  $g(x_1, x_2, x_3, y) \leq 0$  and  $h(x_1, x_2, x_3, y) = 0$  are inequality and equality constraint equations, respectively, with dimensions  $p$  and  $q$ , respectively.

PSO initializes a swarm of random particles in the solution space, each particle representing a potential solution to the problem. We assume that the number of particles is the size of the population, and let it be  $N$ . At the same time, we set the position of the  $l$ th particle in the  $k$ -dimensional solution space as  $x_i = (x_{i1}, x_{i2}, x_{i3}, \dots, x_{ik})^T$  and all have a flying speed as  $v_i = (v_{i1}, v_{i2}, v_{i3}, \dots, v_{ik})^T$ . We judge the pros and cons of the current position according to the fitness function of the particle at the current moment. Subsequently, we update the velocities and positions of the particles themselves according to their optimal positions  $p_i = (p_{i1}, p_{i2}, p_{i3}, \dots, p_{ik})^T$  and  $p_g = (p_{g1}, p_{g2}, p_{g3}, \dots, p_{gk})^T$  of all particles up to now. The updated formula is shown below [16]:

$$\begin{aligned} v_i^{m+1} &= w^m v_i^m + c_1 r_1^m (p_i^m - x_i^m) + c_2 r_2^m (p_g^m - x_i^m), \\ x_i^{m+1} &= x_i^m + v_i^{m+1}. \end{aligned} \quad (2)$$

Among them,  $l = 1, 2, \dots, N$ .  $l$  is the current number of particle swarm iterations.  $r_1$  and  $r_2$  are random numbers between  $[0, 1]$ , which keep the population diversity.  $c_1$  and  $c_2$  are learning factors, which enable particles to move closer to their own optimal position and the optimal position of the group.  $w$  is the inertia weight, which determines the proportion of particles inheriting the current speed. The parameters of PSO mainly include group size, inertia weight, learning factor, maximum speed, etc.

At present, the commonly used dynamic inertia weight is a linear decreasing weight strategy, as follows:

$$w^m = w_{\max} - (w_{\max} - w_{\min}) * \frac{m}{l_{\max}}. \quad (3)$$

Among them,  $m$  is the current number of iterations,  $W_{\max}$  and  $W_{\min}$  are the initial inertia weight and the inertia weight when the maximum number of iterations is reached and  $l_{\max}$  is the maximum number of iterations.

For processing with 0-1 mutation, 1 proposes the following methods:

$p(x_{k+1}^i = 1) = f(v_k^i)$ , we assume  $f(v_k^i) = \text{sig}(v_k^i) = 1/(1 + \exp(-v_k^i))$ . When the random number  $\delta_k^i$  of  $[0, 1]$  is less than  $\text{sig}(v_k^i)$ , then the binary variable takes the value 1. If  $\delta_k^i$  is greater than or equal to  $\text{sig}(v_k^i)$ , the binary variable takes the value 0. Figure 1 is the structure diagram of the two-layer solution strategy of the algorithm [17].

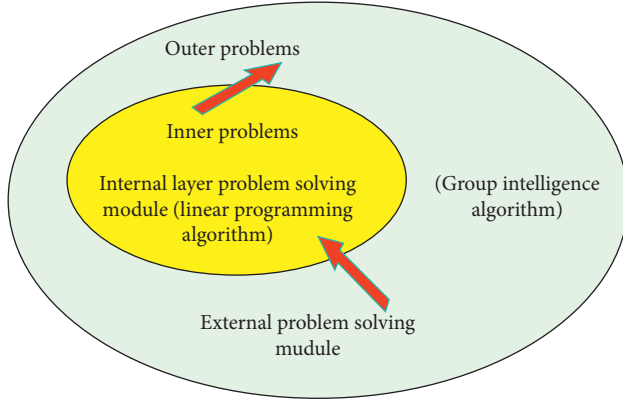
The mixed integer nonlinear programming problem variables include three components: integer variables  $y$ , linear variables  $x_2$ , and nonlinear variables (strong nonlinear variables  $x_1$ , such as exponential logarithmic variables; weak nonlinear variables  $x_3$ , such as double product terms, etc.). We divide these variables into  $L_1$  and  $L_2$ , which correspond to the outer IPSO algorithm and the inner SIM algorithm, respectively. The division strategies are as follows:

- (1) In this study, the integer variable  $y$  and the strong nonlinear continuous variable  $x_1$  are divided into  $L_1$  and the linear continuous variable  $x_2$  is divided into  $L_2$ .
- (2) This study divides the remaining multiple weak nonlinear continuous variables  $x_3$  into  $L_1$  one by one, and observes the remaining  $x_3$ . If the remaining  $x_3$  existence variables become linear variables, they are divided into  $L_2$ , and  $x_3$  is divided into  $L_2$  as much as possible. We assume that  $x_3$  is assigned to the variable  $x_{3L_2}$  in  $L_2$ , and the number of variables is  $l_{3L_2}$ , and the variable assigned to  $L_1$  is  $x_{3L_1}$  and the number of variables is  $l_{3L_1}$ . After grouping there are:

$$\begin{aligned} L_1 &= \{x_1, x_{3L_1}, y\}, \\ L_2 &= \{x_2, x_{3L_2}\}. \end{aligned} \quad (4)$$

Among them, we assume that the number of  $L_2$  variables is  $m_1$  and the number of  $L_1$  variables is  $m_2$ , then there are  $m_1 = l_1 + l_4 + l_{3L_1}$ ,  $m_2 = l_2 + l_{3L_2}$ .

**3.1. Introduce Double Fitness Function.** In this study, dual fitness functions and the tolerance of the system for particles



Mixed-integer nonlinear programming problem

FIGURE 1: IPSO-SIM double-layer zero solution strategy structure.

that do not meet the constraints (default particles) are introduced into IPSO to solve a large number of constraint problems with equations. Among them, the dual fitness functions are  $f_{1,l}^m$  and  $f_{2,l}^m$ , and the tolerance of the system to default particles is  $g$ .

$f_{1,l}^m$  is the improved objective function and  $f_{2,l}^m$  is the default value function of the defined particle, which is defined as follows [18]:

$$f_{1,l}^m = f(x_{1,l}, x_{2,l}, x_{3,l}, y_l),$$

$$f_{2,l}^m = \sum_{i=0}^{p_1} (k_{g,l} * \max(g(L_{1,l}), 0)) + \sum_{i=0}^{q_1} (k_{h,l} * \max|h(L_{1,l})|). \quad (5)$$

Among them,  $m$  is the current number of iterations,  $g(L_1) \leq 0$  is the inequality constraint equation system including the  $L$  variable, the number of equations is  $p_1$ ,  $k_{g,t}$  is the default coefficient of the inequality constraint equation system,  $h(L_1) = 0$  is the equality constraint equation system including  $L$  variable, the number of equation system is  $q_1$ , and  $k_{h,t}$  is the default coefficient of the equality constraint equation system.

In this article, the Deb criterion is improved, and the functional representation of the system tolerance is given. The improved criterion is as follows:

When  $f_{2,l_2}^m \leq g$  and  $f_{2,l_2}^m \leq g$  are satisfied, the smaller particle in the  $f_{1,l_1}^m$  and  $f_{1,l_2}^m$  slips is better. Otherwise, the smaller particle in  $f_{2,l_1}^m$  and  $f_{2,l_2}^m$  is better. Among them,  $g$  is the tolerance of the system to the default particle, and the iterative formula is as follows:

$$g^m = \left( \frac{2 + \alpha}{3 + s/N} - \frac{2 + \alpha}{3} * \frac{m}{M} \right) * g^{m-1} + \delta. \quad (6)$$

Among them,  $s$  is the number of particles with  $f_2^m > 0$ ,  $\alpha$  is the set value, and  $\delta$  is a small positive number.

**3.2. Introduce Linear Robustness.** We assume that the mathematical description of the single-objective optimization problem is as follows:

$$\begin{aligned} & \text{Maximize } f(x, c) \\ & \text{subject to: } x \in S. \end{aligned} \quad (7)$$

Among them,  $x$  is the design parameter,  $c$  is the multidimensional environment parameter, and  $S$  is the dimensional search space. If the optimization process is disturbed by parameter 5, the corresponding objective function value will change from the original  $f(x)$  to  $f(x + \delta)$ . If Maximize: is still a feasible solution, and the variation of the objective function  $\Delta f = f(x + \delta) - f(x)$  falls within the acceptable range, it is called robustness.

For a single-objective optimization problem shown in (8), the curve of  $f(x)$  versus  $x$  is shown in Figure 2. We assume that  $A = (0.3500, 1.2000)$  and  $B = (0.849894, 0.9853)$  are the local and global optimal solutions of the optimization problem, respectively. It can be seen from the figure that if a perturbation  $\delta$  is applied to solution  $A$  and solution  $B$ , respectively (the maximum value of the perturbation does not exceed 0.3), then the influence of the objective function of point  $A$  on the resistance to the movement  $\Delta f_A = f(x_A + \delta) - f(x_A)$  is small. However, the objective function of point  $B$  has a greater influence on the disturbance  $\Delta f_B = f(x_B + \delta) - f(x_B)$ . Therefore, the robustness of point  $A$  is stronger than the bridle of point  $B$ . If  $A$  is outside the acceptable range, then  $A$  is the robust optimal solution to the optimization problem.

$$\begin{aligned} & \text{Maximize: } f(x) = 1 - 0.8e^{-\left(\frac{x-0.35}{0.25}\right)^2} - e^{-\left(\frac{x-0.85}{0.03}\right)^2} \\ & \text{subject to: } x \in [0, 1]. \end{aligned} \quad (8)$$

Therefore, we consider the robustness of the solution and determine the uncertain set of  $x_l = [x_{1,l}, x_{3L_1,l}]^T$  as follows:

$$D_{x_l}^m = \{x_l^m | x_l^m \in [\bar{x}_l^m - e_1, \bar{x}_l^m + e_2]\}. \quad (9)$$

Among them,  $\bar{x}_l^m$  is the nominal value, and  $e_1$  and  $e_2$  are the uncertainties. When calculating the improved objective function of the particle at the  $m$ th iteration, we randomly select the parameter  $C$  times in the uncertain set of  $x_l$  and calculate the mean value as the improved objective function value of each particle, as follows:

$$f_{1,l}^m = \frac{1}{C} \sum_{j=1}^C f_{1,l}^m(x_{i,j}^m). \quad (10)$$

Among them,  $x_{i,j}^m$  is the random value of  $D_{x_l}^m$  in the uncertain set.

This study introduces the role of the robustness of the solution. In view of the parameter fluctuations existing in the industry, some sharp points with poor robustness in the solution space are excluded.

**3.3. Introduce Particle Mutation Probability Function and Double Mutation Strategy.** The outer IPSO algorithm introduces the particle mutation probability function [19]:

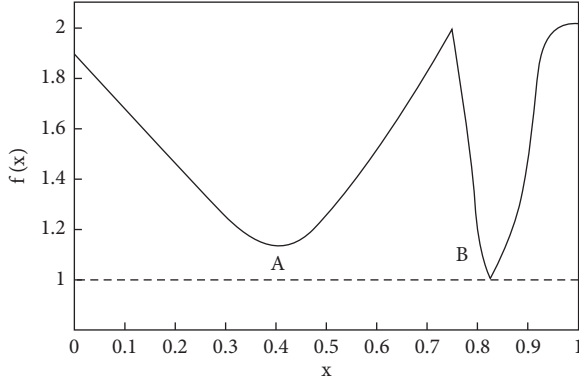


FIGURE 2: Curve over  $[0, 1]$  of the example function.

$$P = \mu + \text{Re} \cdot \sigma. \quad (11)$$

Among them,  $\mu$  and  $\sigma$  are the disturbance rate adjustment parameters, and  $\text{Re}$  is the algebra for which the optimal value of the particle swarm is not obviously optimized. We assume that the optimal value of the  $m-1$  generation particle swarm is  $O(m-1)$ , and the optimal value of the  $m$ th generation particle swarm is  $O(m)$ , where  $m > 1$ . If  $|O(m) - O(m-1)| \leq \varepsilon$ , where  $\varepsilon$  is the threshold variable of the obvious change of the optimal value and is a positive number, it means that the optimal value of the  $m$ th generation particle swarm is not significantly optimized, and  $\text{Re} = \text{Re} + 1$ . If  $|O(m) - O(m-1)| > \varepsilon$ , it means that the optimal value of the  $m$ th generation particle swarm is obviously optimized, and  $\text{Re} = 0$ .

The improved particle swarm algorithm updates the particle's own optimal position  $p\text{Best}$  and the group's optimal position  $g\text{Best}$  each time, and then compares  $P$  with the random value  $\text{Pr}$  in  $(0, 1)$ . When  $\text{Re}$  increases continuously, the probability that  $P$  is greater than the random value  $\text{Pr}$  will increase. When  $P \geq \text{Pr}$ , we save the current  $g\text{Best}$  and perform particle mutation as follows:

Particle mutation is a double mutation strategy, namely particle mutation strategy 1 and particle mutation strategy 2.  $\text{Re}_{p1}$  is the algebra that the optimal value is not obviously optimized after the particle goes through the mutation strategy 1, and  $M_{p1}$  is the threshold value, which is used for the selection of mutation strategy.  $\text{Re}_{p2}$  is the number of times the particle goes through mutation strategy 2, and  $M_{p2}$  is the threshold.

When  $\text{Re}_{p1} \leq M_{p1}$ , particle mutation selects mutation strategy 1, as follows:

$$V_l^m = V_l^m + V_l^m \cdot \alpha_{1v} \cdot \theta \cdot \frac{(M-m)}{M}, \quad (12)$$

$$L_{1,l}^m = L_{1,l}^m + L_{1,l}^m \cdot \alpha_{1L} \cdot \theta \cdot \frac{(M-m)}{M}.$$

Among them,  $V_l^m$  is the velocity of the first particle,  $L_{1,l}^m$  is the position of the first particle,  $L_{1,l}^m$  is the velocity variation coefficient of mutation strategy 1,  $L_{1,l}^m$  is the position variation coefficient of mutation strategy 1,  $m$  is the current number of iterations,  $M$  is the total number of iterations, and

$\theta$  is a random number that obeys the standard normal distribution  $N(0,1)$ .

When  $\text{Re}_{p1} > M_{p1}$ , particle mutation selects mutation strategy 2, as follows:

$$V_l^m = \alpha_{2v} \cdot \theta \cdot \frac{(M-m)}{M}, \quad (13)$$

$$L_{1,l}^m = L_{1,g\text{Best}}^m + \alpha_{2L} \cdot \theta \cdot \frac{(M-m)}{M}.$$

Among them,  $\alpha_{2v}$  is the velocity variation coefficient of mutation strategy 2,  $\alpha_{2v}$  is the position variation coefficient of mutation strategy 2, and  $L_{1,g\text{Best}}^m$  is the position of the global optimal particle. After the particle goes through mutation strategy 2,  $\text{Re}_{p1}$  is reset to 0 and  $\text{Re}_{p2} = \text{Re}_{p2} + 1$ .

After the particle mutates, it enters the inner layer and uses the linear programming algorithm of the inner layer problem-solving module to solve the parameter  $L_{2,l}^m$ . Then, the fitness of the particle swarm is recalculated, the optimal position  $p\text{Best}$  of the particle itself and the optimal position  $g\text{Best}$  of the group are updated, and the particle with the worst fitness is replaced by the backup  $g\text{Best}$ , and  $\text{Re}$  is reset to 0.

We assume that the optimal value of the  $m-1$  generation particle swarm is  $O(m-1)$ . After the particle mutation of the  $m$ th generation particle swarm occurs, the optimal value is  $O(m)$ . If  $|O(m) - O(m-1)| \leq \varepsilon$ , it means that the optimal value of the particle swarm is not significantly optimized after particle mutation,  $\text{Re}_{p1} = \text{Re}_{p1} + 1$ . If  $|O(m) - O(m-1)| > \varepsilon$ , it means that the optimal value of the particle swarm is obviously optimized after particle mutation,  $\text{Re}_{p1} = 0$ .

Combined with the flow chart of the improved particle swarm algorithm and simplex algorithm shown in Figure 3, the specific algorithm steps are as follows:

*Step (1).* In this study, the variables in the mixed integer nonlinear programming problem are divided into two parts, namely  $L_1$  and  $L_2$ , which correspond to the outer simplified mixed integer nonlinear problem and the inner linear programming problem, respectively.

*Step (2).* The outer IPSO algorithm is initialized: we assume that the initial population is  $N$ , the total number of iterations is  $M$ , and the velocity boundary  $[V_{\min}, V_{\max}]$  and position boundary  $[L_{1\min}, L_{1\max}]$  are determined.  $N$  particles uniformly generate the initial position  $L$  in the  $m1$  dimension and randomly generate the initial velocity  $V_l^0$ , where  $l = 1, \dots, N$ .

*Step (3).* The  $L_1$  parameter is fixed to  $L_{1,l}^m$  by IPSO, and the problem is transformed into a linear programming problem. Then, it enters the inner layer and uses the linear programming algorithm of the inner layer problem-solving module to solve the parameter  $L_2$ , the solution of the parameter  $L_2$  is denoted as  $L_{2,l}^m$ , where  $m$  is the current iteration number, and the initial solution is denoted as  $L_{2,l}^0$ .

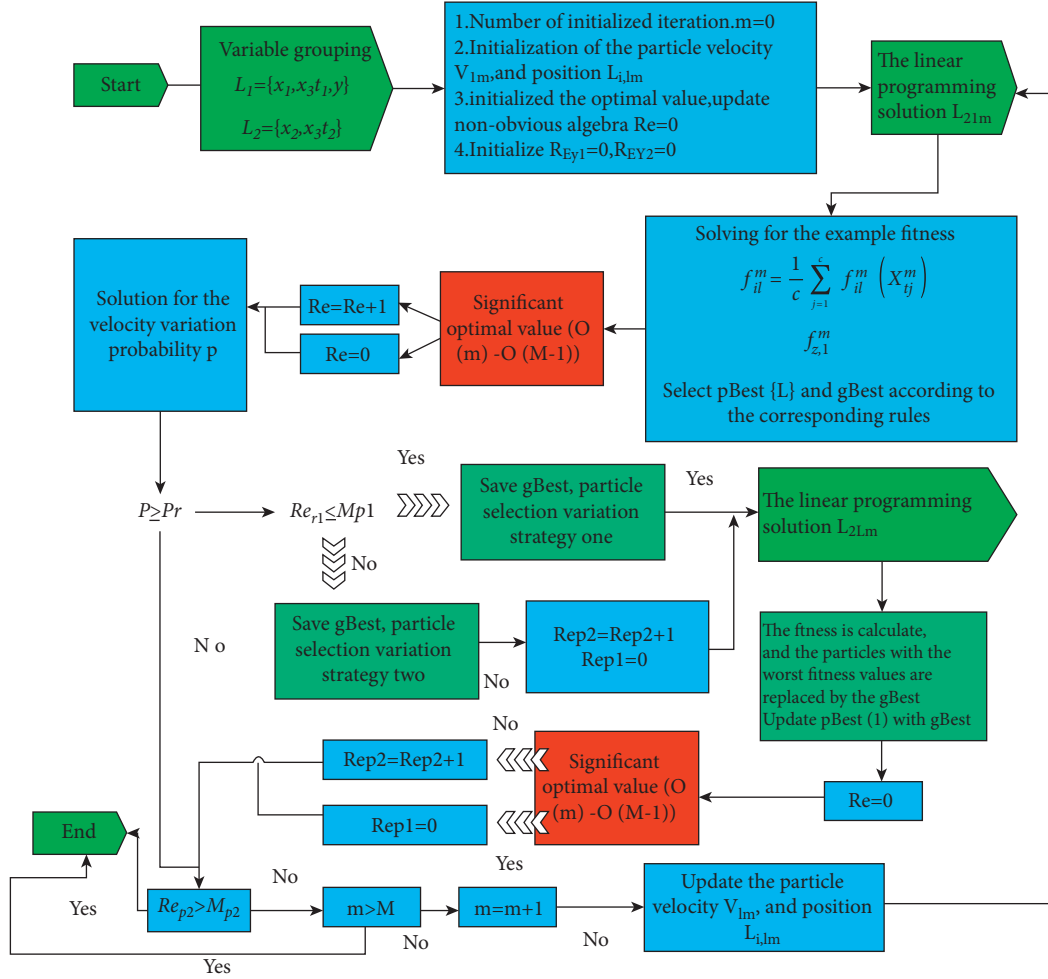


FIGURE 3: Flow chart of improved particle swarm algorithm and simplex algorithm (IPSO-SIM).

Step (4). The outer IPSO algorithm calculates  $f_{1,l}^m$  and  $f_{2,l}^m$  considering the robustness of the solution according to  $[L_{1,l}^m, L_{2,l}^m]$ , and updates the optimal position  $pBest^m[l]$  of the particle itself and the optimal position  $gBest^m$  of the group;

Step (5). In this study, the particle mutation probability function value  $P$  of the population is calculated and compared with the random value  $Pr$  in  $(0, 1)$ . If  $P \geq Pr$ , particle mutation is performed on the population, and the mutation strategy is selected according to  $Re_{p1} \leq Mp_{p1}$ . If we choose mutation strategy 1, then we use equations (10) and (11) to get the mutated  $L_{1,l}^m$ . If  $V_l^m$  chooses mutation strategy 2, then we use equations (12) and (13) to obtain the mutated  $L_{1,l}^m$  and  $V_l^m$ , reset  $Re_{p1}$  and set  $Re_{p2} = Re_{p2} + 1$ . Then,  $L_{2,l}^m, f_{1,l}^m, f_{2,l}^m, pBest^m[l]$  are retrieved. If  $P < Pr$ , we go directly to step (6).

Step (6). This study judges whether the termination condition  $m > M$  or  $Re_{p2} \geq Mp_{p2}$  is satisfied, where  $M_{pz}$  is the threshold number of times to execute particle perturbation strategy 2,  $2 \leq Mp_{p2} \leq M$ . If none of the termination conditions are satisfied, then  $m = m + 1$ . According to the optimal position  $pBest[l]$  of the particle itself and the optimal position  $gBest$  of the group, and according to the standard

particle swarm algorithm, the velocity  $v_l^m$  and the position  $L_{1,l}^m$  are updated, and return to step (2). If any of the termination conditions are met, the algorithm ends.

#### 4. Coordinated Operation Scheduling Model of Agricultural Machinery Based on Particle Swarm Neural Network

The traveling salesman problem (TSP) is a typical NP-complete problem in combinatorial optimization problems. It means that the distance between  $n$  cities and each pair of cities is given, and each city can be visited only once, and the shortest path that can return to the departure city is solved. This study applies it to the path scheduling of agricultural machinery, and the traveling salesman problem is shown in Figure 4(a).

The vehicle routing problem (VRP) is one of the most fundamental problems in network optimization. The problem is that at a station,  $M$  trucks and  $N$  customers are given, where the vehicle capacity is  $Q$ , and the demand for each customer is  $D$ . Vehicles depart from the depot for delivery services and finally return to the depot. It is restricted that all customers are delivered, and each customer

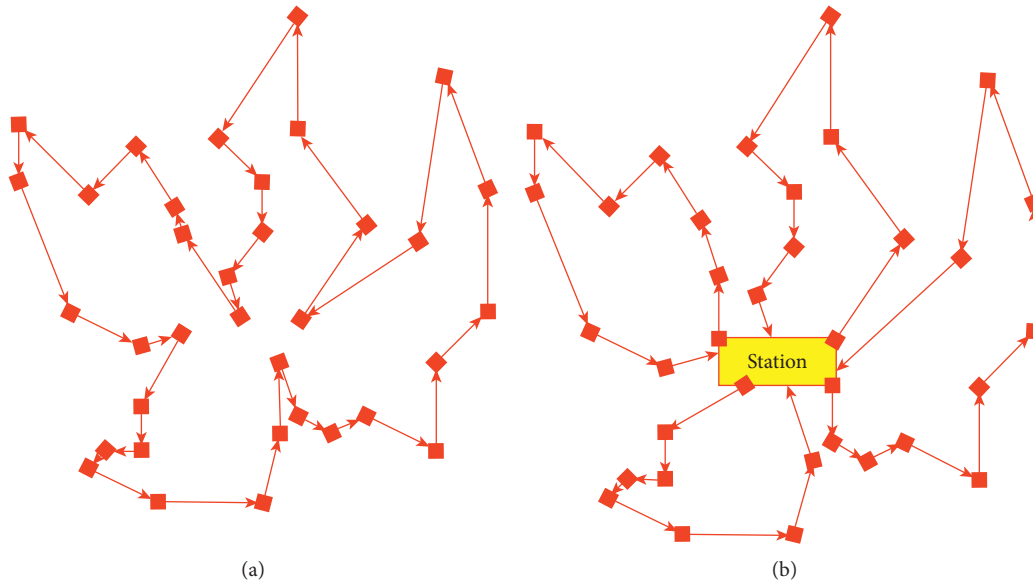


FIGURE 4: Research on agricultural path problem. (a) Schematic diagram of the traveling salesman problem. (b) Schematic diagram of agricultural machinery routing problem.

is delivered at one time, and the vehicle capacity cannot be exceeded, and the goal is to minimize the total distance of the delivery route. Figure 4(b) shows the schematic diagram of the agricultural machinery path problem.

In order to ensure that the difference between the maximum value and the minimum value of the total field area in each cluster does not exceed 2000 mu (one day's work volume), when each field block is added to a certain cluster, the total work area is calculated. If it is larger than the total working area, a sacrifice field is ejected. Figure 5 shows the flow chart of the improved program.

The agricultural machinery monitoring system mainly includes three modules: agricultural machinery terminal, communication network, and dispatching center. The system framework is shown in Figure 6:

The monitoring center mainly includes three parts: server, database, and client. Among them, the communication server is mainly connected with the agricultural machinery terminal through the GPRS network, and its main job is to store the received relevant data from the agricultural machinery terminal in the database and also send the corresponding scheduling information to the agricultural machinery terminal. The web server is connected to the client through the Internet network, and its main function is to analyze and respond to the request sent by the client in time, including extracting the real-time positioning data of agricultural machinery from the corresponding database and then returning the data to the client, etc. The agricultural machinery dispatching system is shown in Figure 7(a) and the realized function is shown in Figure 7(b).

To design the communication protocol of the system, the first step is to analyze the business data flow of the system. Figure 8 is a system data flow diagram. The monitoring data of the system are mainly collected and generated by the sensor network and the monitoring circuit of the front-end controller, and the control data are generated by the

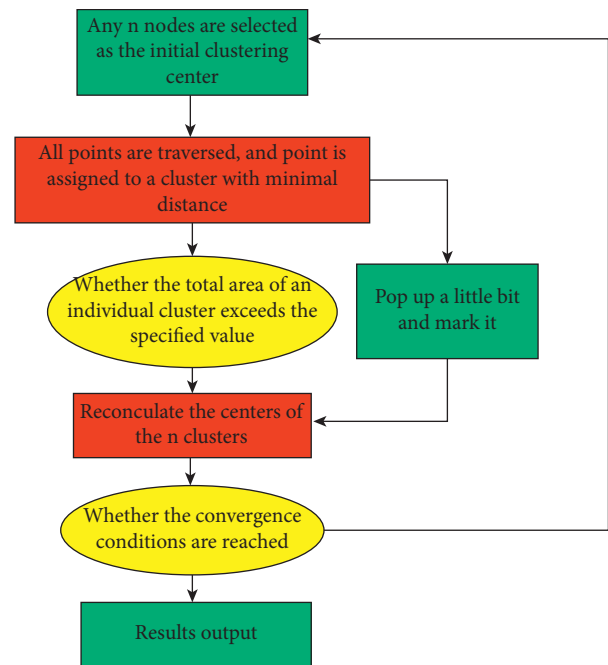


FIGURE 5: Program flow chart.

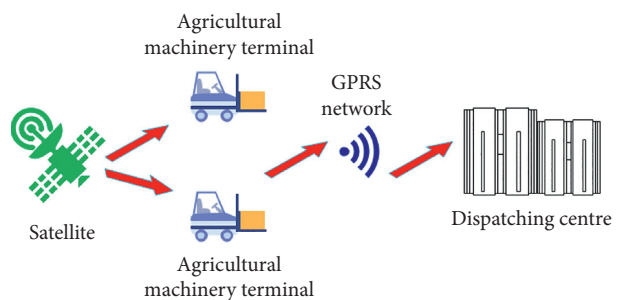


FIGURE 6: System framework.

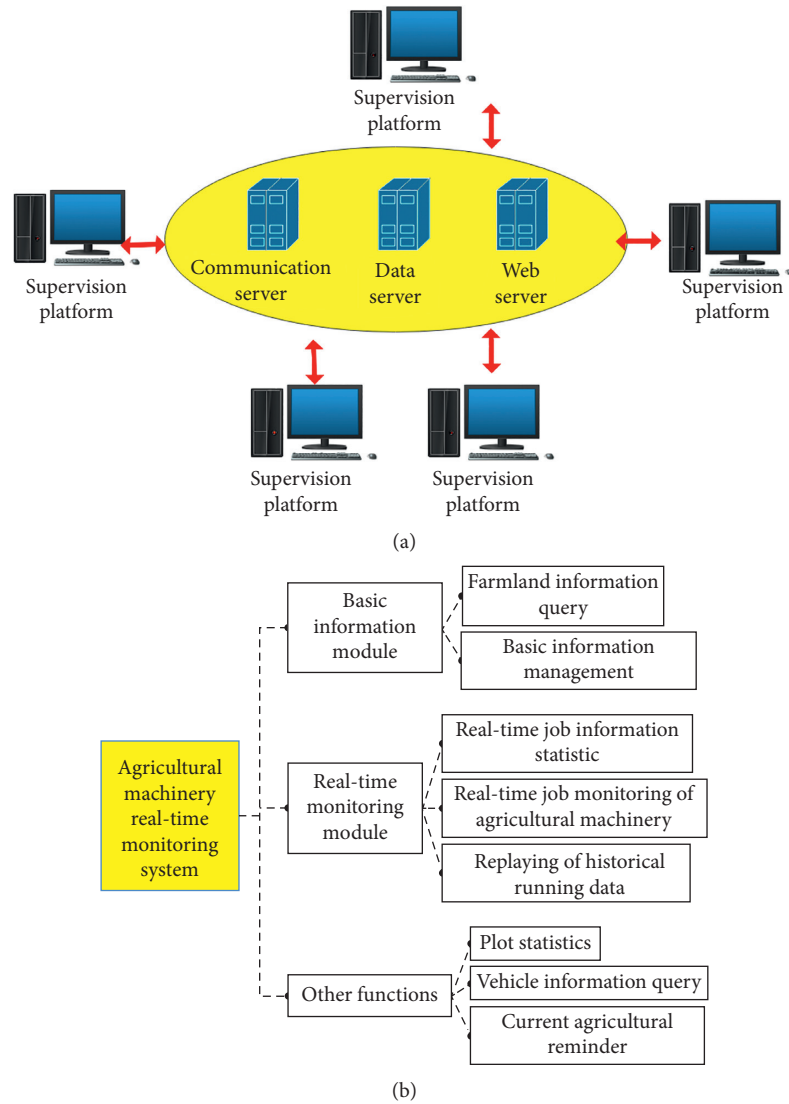


FIGURE 7: Agricultural machinery scheduling system. (a) Structure diagram of monitoring center. (b) Functional block diagram.

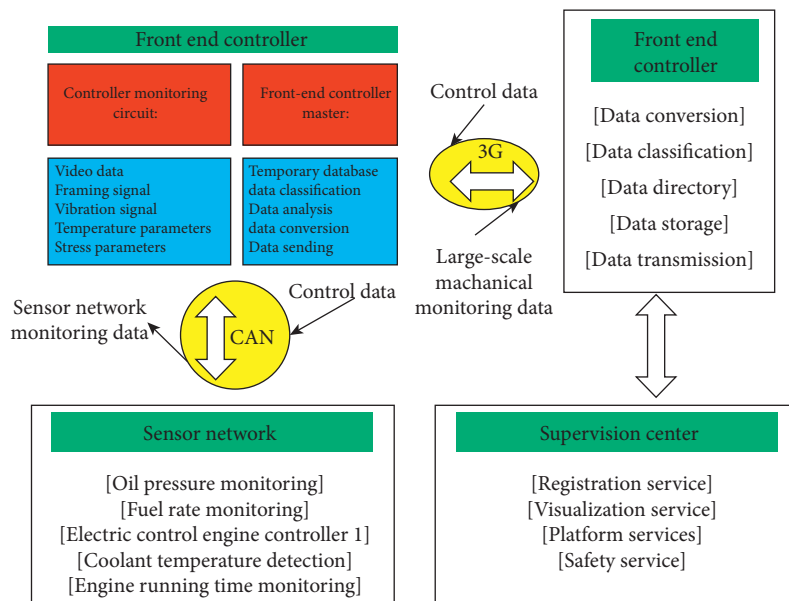


FIGURE 8: System data flow diagram.



TABLE 1: Data processing effect of agricultural machinery cooperative operation scheduling system based on particle swarm neural network.

| Number | Agricultural data processing | Number | Agricultural data processing | Number | Agricultural data processing |
|--------|------------------------------|--------|------------------------------|--------|------------------------------|
| 1      | 95.02                        | 28     | 93.81                        | 55     | 92.12                        |
| 2      | 95.18                        | 29     | 95.45                        | 56     | 95.67                        |
| 3      | 95.52                        | 30     | 93.75                        | 57     | 94.64                        |
| 4      | 93.71                        | 31     | 95.67                        | 58     | 93.59                        |
| 5      | 93.89                        | 32     | 92.36                        | 59     | 93.97                        |
| 6      | 93.29                        | 33     | 94.97                        | 60     | 93.65                        |
| 7      | 95.60                        | 34     | 93.28                        | 61     | 93.86                        |
| 8      | 95.87                        | 35     | 95.99                        | 62     | 92.82                        |
| 9      | 95.23                        | 36     | 94.80                        | 63     | 92.69                        |
| 10     | 92.83                        | 37     | 93.18                        | 64     | 94.00                        |
| 11     | 94.64                        | 38     | 94.87                        | 65     | 92.32                        |
| 12     | 93.92                        | 39     | 93.01                        | 66     | 95.68                        |
| 13     | 95.24                        | 40     | 94.90                        | 67     | 95.23                        |
| 14     | 93.02                        | 41     | 92.87                        | 68     | 94.03                        |
| 15     | 94.72                        | 42     | 93.87                        | 69     | 92.18                        |
| 16     | 94.21                        | 43     | 92.89                        | 70     | 92.91                        |
| 17     | 95.16                        | 44     | 95.13                        | 71     | 93.07                        |
| 18     | 93.59                        | 45     | 92.05                        | 72     | 93.21                        |
| 19     | 93.32                        | 46     | 94.25                        | 73     | 94.39                        |
| 20     | 95.60                        | 47     | 93.79                        | 74     | 93.43                        |
| 21     | 95.72                        | 48     | 95.57                        | 75     | 94.09                        |
| 22     | 93.59                        | 49     | 92.71                        | 76     | 95.65                        |
| 23     | 92.17                        | 50     | 92.86                        | 77     | 95.46                        |
| 24     | 93.57                        | 51     | 95.14                        | 78     | 93.34                        |
| 25     | 93.13                        | 52     | 92.93                        | 79     | 95.28                        |
| 26     | 95.80                        | 53     | 94.24                        | 80     | 92.08                        |
| 27     | 94.36                        | 54     | 93.86                        | 81     | 95.98                        |

TABLE 2: Operation scheduling effect of agricultural machinery cooperative operation scheduling system based on particle swarm neural network.

| Number | Collaborative work | Number | Collaborative work | Number | Collaborative work |
|--------|--------------------|--------|--------------------|--------|--------------------|
| 1      | 88.82              | 28     | 87.00              | 55     | 88.90              |
| 2      | 88.82              | 29     | 83.60              | 56     | 86.27              |
| 3      | 82.49              | 30     | 86.48              | 57     | 89.76              |
| 4      | 88.53              | 31     | 87.70              | 58     | 82.92              |
| 5      | 88.37              | 32     | 84.03              | 59     | 88.66              |
| 6      | 86.85              | 33     | 89.87              | 60     | 83.84              |
| 7      | 87.52              | 34     | 84.40              | 61     | 82.44              |
| 8      | 81.46              | 35     | 89.07              | 62     | 86.05              |
| 9      | 82.01              | 36     | 89.60              | 63     | 87.17              |
| 10     | 90.83              | 37     | 81.05              | 64     | 81.88              |
| 11     | 86.65              | 38     | 81.72              | 65     | 86.39              |
| 12     | 85.95              | 39     | 82.52              | 66     | 90.61              |
| 13     | 90.14              | 40     | 88.12              | 67     | 90.94              |
| 14     | 85.15              | 41     | 85.20              | 68     | 85.30              |
| 15     | 86.05              | 42     | 84.69              | 69     | 85.72              |
| 16     | 83.51              | 43     | 89.81              | 70     | 80.81              |
| 17     | 82.33              | 44     | 87.92              | 71     | 84.97              |
| 18     | 90.80              | 45     | 86.27              | 72     | 86.29              |
| 19     | 80.29              | 46     | 86.60              | 73     | 82.45              |
| 20     | 82.08              | 47     | 87.31              | 74     | 81.50              |
| 21     | 85.74              | 48     | 90.06              | 75     | 83.84              |
| 22     | 81.74              | 49     | 80.71              | 76     | 82.00              |
| 23     | 87.37              | 50     | 88.24              | 77     | 88.44              |
| 24     | 85.28              | 51     | 81.98              | 78     | 86.28              |
| 25     | 81.36              | 52     | 87.70              | 79     | 85.58              |
| 26     | 90.27              | 53     | 87.68              | 80     | 80.43              |
| 27     | 85.70              | 54     | 80.98              | 81     | 86.91              |

monitoring center. As the data preprocessing center of the system, the front-end controller plays the role of a data hub in the entire monitoring system.

Based on the above research, this study combines the simulation test to verify the effect of the agricultural machinery cooperative operation scheduling model based on the particle swarm neural network constructed in this study. Moreover, this study counts the agricultural machinery collaborative data processing effect and operation scheduling effect of this system, and the statistical results are shown in Tables 1 and 2.

From the above research, it can be seen that the cooperative operation scheduling model of agricultural machinery based on particle swarm neural network proposed in this study can play an important role in modern agricultural planting and effectively improve the efficiency of agricultural planting.

## 5. Conclusion

For those who demand agricultural machinery services, such as contracted land managers and individual farmers, it is neither realistic nor economical to purchase agricultural machinery by themselves, but they have an urgent need for agricultural machinery operations. The agricultural machinery service demander publishes its own operation requirements, including constraints on the operation plot, operation type, and operation time. In the face of a large number of operational demands, agricultural machinery service providers combine the existing agricultural machinery resources to allocate appropriate agricultural machinery for each farmland operation and plan appropriate driving routes for each agricultural machinery, so as to maximize the utilization of resources. This new agricultural machinery operation mode derives a new research topic, namely the agricultural machinery scheduling problem studied in this article. This article combines the particle swarm neural network to study the cooperative operation scheduling algorithm of agricultural machinery to improve the cooperative scheduling effect of intelligent agricultural machinery. The research shows that the cooperative operation scheduling model of agricultural machinery based on particle swarm neural network proposed in this article can play an important role in modern agricultural planting and effectively improve the efficiency of agricultural planting.

## Data Availability

The labeled dataset used to support the findings of this study are available from the corresponding author upon request.

## Conflicts of Interest

The author declares no competing interests.

## Acknowledgments

This study was sponsored by Jiangsu Food and Pharmaceutical Science College.

## References

- [1] S. L. Luo, M. He, and J. Y. Li, "Fuzzy comprehensive evaluation method calculation of correlation degree and module division of agricultural machinery parts," *Journal of Agricultural Science and Technology A*, vol. 21, no. 2, pp. 71–81, 2019.
- [2] E. M. C. Cárdenas, V. D. B. Morocho, and E. P. A. Pérez, "Design and manufacture of protective elements to prevent accidents in the agricultural machinery of Ecuador, two cases of study in automotive elements," *Ciencia Digital*, vol. 2, no. 3, pp. 187–202, 2018.
- [3] L. Ma, M. Iqbal, and K. Cengiz, "Realization of agricultural machinery equipment management information system based on network," *International Journal of Agricultural and Environmental Information Systems*, vol. 12, no. 3, pp. 13–25, 2021.
- [4] V. Pryshliak, "Theory OF project preparation OF agro-engineers ON the basis OF scientific work ON the development OF agricultural machinery," *Science. Business. Society*, vol. 3, no. 4, pp. 145–149, 2018.
- [5] B. Pişkin and R. Sağlam, "The important role of retrofitting in agricultural machinery: a case study for techniques and applications," *Geotekhnicheskaya Mekhanika*, vol. 16, no. 133, pp. 114–122, 2017.
- [6] F. K. Abagale, "Effect of agricultural machinery on physical and hydraulic properties of agricultural soils," *Journal of Soil Science and Environmental Management*, vol. 12, no. 2, pp. 58–65, 2021.
- [7] M. Bebeti, N. Feuchtner, and M. Klaffenböck, "100% electric-drive for compact construction and agricultural machinery," *ATZheavy duty worldwide*, vol. 14, no. 1, pp. 10–15, 2021.
- [8] M. Bietresato and F. Mazzetto, "Increasing the safety of agricultural machinery operating on sloping grounds by performing static and dynamic tests of stability on a new-concept facility," *International journal of safety and security engineering*, vol. 8, no. 1, pp. 77–89, 2018.
- [9] M. Javaid and A. Haleem, "Using additive manufacturing applications for design and development of food and agricultural equipments," *International Journal of Materials and Product Technology*, vol. 58, no. 2-3, pp. 225–238, 2019.
- [10] P. Q. Tan, D. Y. Wang, and D. M. Lou, "Progress of control technologies on exhaust emissions for agricultural machinery," *Transactions of the Chinese Society of Agricultural Engineering*, vol. 34, no. 7, pp. 1–14, 2018.
- [11] Z. Liu, Z. Zhang, and X. Luo, "Design of automatic navigation operation system for Lovol ZP9500 high clearance boom sprayer based on GNSS," *Transactions of the Chinese Society of Agricultural Engineering*, vol. 34, no. 1, pp. 15–21, 2018.
- [12] X. Qin, D. Jiang, and L. Pretorius, "The impact of financial factors on the after-sales service of agricultural machinery: a case study of Chinese agricultural machinery in South Africa," *Asian Journal of Agriculture and Rural Development*, vol. 11, no. 1, pp. 71–78, 2021.
- [13] N. A. Ivanov, D. V. Otmakhov, D. V. Otmakhov, S. P. Zakharychev, and O. V. Kazannikov, "Development of the design of an internal combustion engine cooling system with a pre-starting heating function," *Traktory i sel'hozmas-shiny*, vol. 1, no. 1, pp. 51–56, 2021.
- [14] Y. Zhao, X. Zheng, and X. Chen, "Design and test of CMJY-1 500 type plastic film residue collecting and balling machine," *Transactions of the Chinese Society of Agricultural Engineering*, vol. 33, no. 5, pp. 1–9, 2017.

- [15] Z. A. Godzhaev, A. Y. U. Izmajlov, and Y. U. F. Lachuga, "Prospects for the use of automated and robotized electric drives on mobile energy equipment and agricultural machinery working bodies," *Izvestiya MGTU MAMI*, vol. 7, no. 2, pp. 41–47, 2018.
- [16] Y. Che, L. Wei, and X. Liu, "Design and experiment of seeding quality infrared monitoring system for no-tillage seeder," *Transactions of the Chinese Society of Agricultural Engineering*, vol. 33, no. 1, pp. 11–16, 2017.
- [17] L. Zheng, "Optimization of agricultural machinery task scheduling algorithm based on multiobjective optimization," *Journal of Sensors*, vol. 2022, Article ID 5800332, 12 pages, 2022.
- [18] S. Dong, Z. Yuan, and C. Gu, "Research on intelligent agricultural machinery control platform based on multi-discipline technology integration," *Transactions of the Chinese Society of Agricultural Engineering*, vol. 33, no. 8, pp. 1–11, 2017.
- [19] S. H. Zhao, H. J. Liu, and H. W. Tan, "Design and experiment of bidirectional profiling press device for hilly area," *Transactions of the Chinese Society for Agricultural Machinery*, vol. 48, no. 4, pp. 82–89, 2017.